Eur Biophys J (2003) 32: 33–39
DOI 10.1007/s00249-002-0270-y

ARTICLE

**Robert W. Stark · Francisco J. Rubio-Sierra
Stefan Thalhammer · Wolfgang M. Heckl**

Combined nanomanipulation by atomic force microscopy and UV-laser ablation for chromosomal dissection

Received: 24 May 2002 / Accepted: 11 November 2002 / Published online: 28 January 2003

Abstract Nanomanipulation and nanoextraction on a scale close to and beyond the resolution limit of light microscopy is needed for many modern applications in biological research. For the manipulation of biological specimens a combined microscope allowing for ultraviolet (UV) microbeam laser manipulation together with manipulation by an atomic force microscope (AFM) was used. In a one-step procedure, human metaphase chromosomes were dissected optically by the UV-laser ablation and mechanically by AFM manipulation. With both methods, sub-400-nm cuts could be achieved routinely. Thus, the AFM is an indispensable tool for in situ quality control of nanomanipulation. However, already on this scale the dilation of the topographic AFM image due to the tip geometry can become significant. Therefore the AFM images were restored using a tip geometry obtained by a blind tip-reconstruction algorithm. Cross-sectional analysis of the restored image reveals a 380-nm-wide UV-laser cut and AFM cuts between 70 nm and 280 nm.

Keywords Image processing · Ultraviolet lasers · Scanning force microscopy · Microdissection

Introduction

Nanotechnology offers the prospect of analyzing, handling and manipulating biological objects on the nanometer scale. For instance, elastic properties of single DNA molecules can be investigated by means of laser methods: optical microdissection with an utraviolet (UV) laser microbeam can be used to disrupt the molecule (Endlich et al. 1994). Alternatively, an optical trap can be used to control a microsphere where a DNA molecule is attached (Perkins et al. 1994). Mechanical manipulation using an atomic force microscope (AFM) provides complementary information. Controlled nanodissection of DNA by an AFM is possible with high spatial resolution (Henderson 1992; Guthold et al. 1999), as well as the mechanical manipulation of the DNA molecule for the investigation of elastic properties (Krautbaur et al. 2000). These examples illustrate the potential of the fundamentally different approaches for manipulation on the smallest scales: optical methods employing different types of lasers and mechanical methods based on the AFM.

An important application of manipulation and extraction in biological applications is the recovery of DNA by chromosomal dissection for cytogenetic studies, like chromosome-specific molecular analysis of genes, studies of chromosomal evolution or the investigation of genetic defects. Already in the 1960s, optical manipulation of chromosomes was shown with a pulsed argon laser microbeam (Berns et al. 1969). Later, collection of the chromosomal DNA by UV-laser catapulting for further amplification by a degenerate oligonucleotide polymerase chain reaction (PCR) was demonstrated (Schermelleh et al. 1999). Today, manipulation by a UV-laser microbeam is a well-established technique in biomedical research (e.g. Schütze et al. 1997; Thalhammer et al. 1997a; Clement Sengewald et al. 2000; Greulich et al. 2000). The underlying process of UV-laser manipulation is a locally restricted ablative photodecomposition without heating (Srinivasan 1986). For an overview, see Greulich (1999) and Bäuerle (2000).

Other laser-surgery methods for biomedical research were developed employing IR or near-IR lasers. Emmert Buck and co-workers (1996) reported on successful IR laser manipulation in experiments where the sample was

R.W. Stark (✉) · F.J. Rubio-Sierra · S. Thalhammer
W.M. Heckl
Institut für Kristallographie und Angewandte Mineralogie,
Ludwig-Maximilians-Universität München,
Theresienstrasse 41, 80333 Munich, Germany
E-mail: stark@nanomanipulation.de
Tel.: +41-1-6323402
Fax: +41-1-6321278

Present Address: R.W.Stark
Nanotechnology Group, ETH Zurich,
ETH Center CLA, 8092 Zurich, Switzerland

covered with a thermoplastic film that was locally molten by laser irradiation. After cooling and recrystallization, the specimen in the targeted area adhered to the film and was removed for further processing. With this method, cell fragments with a size of about 10 μm can be extracted (Godstein et al. 1999). So far, this method provides significantly less spatial resolution than UV-laser microdissection. Another promising approach to optical manipulation of biological material is the multiphoton-induced ablation by 800-nm femtosecond laser pulses (König et al. 2001). Complete sub-200-nm cuts can be achieved in fixed air-dried human metaphase chromosomes with this method. Unlike UV-laser ablation, this technique requires several passes with the cutting laser. Up to now the femtosecond laser technique does not provide a direct harvest method and is significantly more cost intensive. Thus, for sub-micron laser microdissection and sample collection in cost-sensitive applications, UV-laser manipulation seems appropriate.

Complementary to laser methods, the AFM offers high-resolution imaging and precise mechanical manipulation capabilities. The applications of the AFM in chromosome research range from the investigation of the structure and organization of the chromatin to manipulation and material extraction for genetic analysis. Topographic AFM imaging of chromosomes with a resolution beyond the diffraction limit of light microscopy was reported by various authors (De Grooth and Putman 1992; Rasch et al. 1993; McMaster et al. 1994; Tamayo et al. 1999; Thalhammer et al. 2001). Moreover, manipulation by mechanical scratching of genetic material with the AFM tip has been demonstrated (Allen et al. 1993; Jondle et al. 1995). After AFM dissection, chromosomal material adheres to the AFM tip (Stark et al. 1998). This DNA can be recovered from the tip and amplified with PCR techniques (Thalhammer et al. 1997a; Xu and Ikai 1998).

Usually, long-distance optics are needed in optical microscopes that are integrated in micromanipulation set-ups to allow for access to the specimen. Thus, the resolution:

$$d = 1.22\lambda / \left(\mathrm{NA_{obj}} + \mathrm{NA_{cond}}\right) \quad (1)$$

of a typical inverted light microscope used in manipulation experiments is limited to about $d \approx 350$ nm (green-light illumination, $\lambda \approx 500$ nm; $\mathrm{NA_{obj}} = 1.20$; $\mathrm{NA_{cond}} = 0.55$). This illustrates that for the analysis of sub-micron laser manipulation and nanometer AFM manipulation a conventional light microscope is not sufficient. In contrast, the resolution of the AFM is limited by the diameter of the scanning tip, which is usually within the range from 5 to 50 nm. Combined instruments unite the resolution of the AFM with the ease of use of the light microscope (Putman et al. 1993; Hillner et al. 1995; Thalhammer et al. 1997b).

However, imaging with an AFM also requires quality control. During AFM imaging the AFM tip can deteriorate owing to hard impacts of the tip on the sample or to pick-up of debris from the sample. Usually, the operator visually assesses the quality of the AFM tip from the image data. As this process highly depends on the experience of the human operator, a less subjective criterion for the quality of the AFM image is desirable. For routine use in biomedical applications, time-consuming tip characterization procedures using standard samples or electron microscopy are too slow. For standard laboratory use, only in situ characterization of the AFM tip is appropriate. This can be achieved by estimation of the tip geometry from tip self-imaging on the sample (van Loenen et al. 1990; Markiewicz and Goh 1995; Fritzsche et al. 1996). The blind tip-reconstruction method (Dongmo et al. 1996; Villarrubia 1997) allows us to assess the tip geometry directly from the image morphology.

In the following, we report on the optical as well as mechanical nanodissection of human metaphase chromosomes in an integrated nanomanipulator without the need to transfer the sample between different instruments. A commercial force-feedback joystick provides a simple but intuitive user interface for manipulation. For quality control of AFM imaging we show that AFM tip characterization is necessary in order to obtain reliable distance measurements.

Materials and methods

Nanomanipulation platform

For dissection as well as for imaging, an integrated nanomanipulation platform was developed that combines optical manipulation with mechanical manipulation. In this instrument, a scanning probe microscope and a UV laser were integrated to an inverted microscope (Axiovert 100, Carl Zeiss, Göttingen, Germany) as shown in Fig. 1a. The epi-illumination path of the light microscope was equipped with quartz glass optics for efficient UV light transmission. For the laser microdissection experiments a 100x Glyc Ultrafluar (Carl Zeiss) objective with numerical aperture $\mathrm{NA_{obj}} = 1.20$ was employed. A long-distance condenser with $\mathrm{NA_{cond}} = 0.55$ (0.55 H, Carl Zeiss) was used for simultaneous AFM and light microscopic measurements. Light microscopic data were recorded with a CCD camera (Photometrics CoolSNAP, Roper Scientific, Trenton, NJ, USA).

The UV-laser microbeam (PALM Microlaser Technologies, Bernried, Germany) for photo-manipulation was coupled into the epi-illumination path. This pulsed nitrogen UV laser ($\lambda = 337.1$ nm) was specified with a pulse width of less than 4 ns (full width at half maximum height) and a pulse energy of 300 μJ with an adjustable pulse repetition rate between 0 and 60 Hz. The laser energy could be attenuated continuously without beam displacement. The commercial laser interface (PALM) allowed for coarse laser focus adjustment, independent of the microscope focus.

The scanning probe microscope (SPM) was a multifunctional system that could be operated as an AFM or scanning near-field optical microscope (Biolyser, Triple-O, Potsdam, Germany). The specimen was scanned with respect to the AFM tip and the optical axis in this SPM design (Fig. 1b). To allow for SPM and laser nanomanipulation as well as for SPM imaging, a separate nanomanipulation control was implemented (Fig. 1c). The nanomanipulation system could be switched between imaging and manipulation mode with this control. The force signal F of the AFM was fed back into the SPM control unit as well as the manipulation control unit. The x, y and z positions of the sample stage were controlled by the original SPM control in imaging mode.

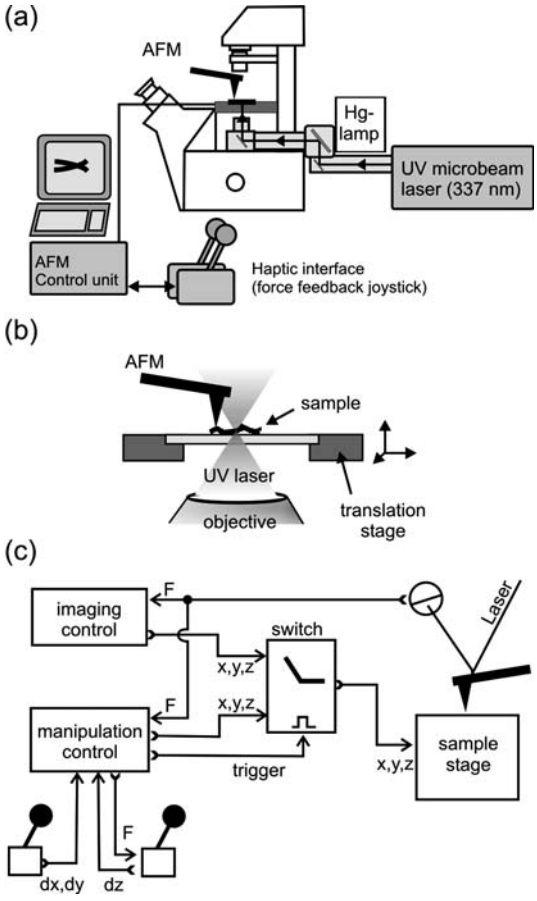

Fig. 1a–c Experimental setup. **a** A multifunctional scanning probe microscope is mounted onto an inverted research microscope. In addition, a pulsed UV microbeam laser is coupled to the microscope through the epi-illumination path. The electronic control unit simultaneously controls laser manipulation and scanning probe microscopy. A force-feedback joystick serves as a simple haptic interface to the SPM. **b** The scanning stage can be positioned with nanometer resolution in three dimensions with piezoelectric actuators, allowing for scanning probe microscopy as well as for laser micromanipulation. **c** Block diagram of the control system

In manipulation mode, the user directly controlled the lateral translation velocity (dx, dy) of the sample stage with a positioning joystick. For intuitive control of the tip force in mechanical manipulation experiments, a commercial force feedback joystick (WingMan Force, Logitech, Fremont, Calif., USA) was implemented as a simple and low-cost haptic interface. With this second joystick the z-position of the sample stage corresponding to the tip force on the sample was controlled by the user. In the photoablation mode the lateral position of the scanning stage was steered with the positioning joystick. The second joystick served for the fine adjustment of the specimen with respect to the laser focus, which was achieved by vertical displacement of the piezoelectric actuators of the scanning stage. A more detailed description of the nanomanipulator can be found elsewhere (Rubio-Sierra et al. 2003).

Imaging and nanomanipulation procedure

SPM data presented here were obtained in AFM mode. The AFM was calibrated prior to the experiments. In order to account for the non-linearity of the open-loop-controlled piezo actuators, a 5% error is assumed for topographical data. Topographic images were obtained in the dynamic intermittent contact mode in the AFM using stiff silicon cantilevers (Pointprobe NCH, Nanosensors Dr. Olaf Wolter, Wetzlar, Germany) with a nominal spring constant $k = 21$–78 N/m and a nominal tip radius of 20 nm. For imaging, the scan rate was limited to 1 Hz.

To optically dissect the specimen the laser energy was adjusted to about 1 μJ/pulse and the sample was moved through the focus by the piezoelectric transducers of the SPM. For mechanical AFM manipulation the same type of cantilever as used for imaging was employed. Dissection was achieved by increasing the loading force of the tip onto the sample while the driving modulation for the dynamic mode of the cantilever base was maintained. This resulted in a modulated contact mode manipulation ensuring precise AFM dissection of the biological material (Stark et al. 1998). Dissection was performed at an average scan speed of 0.5 μm/s. The calibrated spring constant $k = 60 \pm 5$ N/m of the cantilever was obtained following a standard procedure (Sader et al. 1999).

Human metaphase chromosomes

Heparinized human whole blood (0.4 mL) was cultivated at 37 °C for 72 h in 10 mL Gibco Chromosome medium 1A (Invitrogen, Karlsruhe, Germany). Cells were arrested by 30 min colchicine treatment (100 μL) followed by centrifugation (10 min at 1000 rpm). Chromosomes were prepared by resuspending the pellet in 10 mL of 0.075 M KCl and incubation at 37 °C for 15 min. After a further centrifugation (10 min at 1000 rpm) the pellet was carefully resuspended in a freshly prepared mixture of 3:1 methanol/acetic acid at 4 °C and fixed for 25 min at 4 °C. After three washing steps in the methanol/acetic acid fixative the chromosomes were dropped onto 0.17-mm coverslips, rinsed in PBS and air-dried.

The unbanded chromosomes were classified based on the criteria of length and centromere index, i.e. the ratio of the length of the short arm to the chromosome length×100 (Vogel and Motulsky 1997). Both features are considered the most discriminative geometric features of human metaphase chromosomes (Lerner 1998). The error of the centromere index was estimated from the difference between the minimum and maximum acceptable length of the p-arm.

Image processing

Images were analyzed using the SPIP software package (Image Metrology, Lyngby, Denmark). First, the raw data were leveled to remove tilt from the data. In the next step a 3×3 median filter was applied to suppress noise that otherwise would lead to an underestimation of the tip radius in the subsequent procedure. In order to obtain reliable estimates for the cut widths, an image reconstruction was performed. The AFM tips were estimated using a blind tip-reconstruction algorithm (Villarrubia 1997). With this algorithm a "worst case tip" was calculated, i.e. upper constraints for the tip geometry were obtained. This information was then used to restore the AFM image. This procedure did not enhance the resolution but it provided reliable metrological data on surface features like hills that otherwise would have been overestimated in their lateral dimensions and grooves that would have been underestimated.

Results and discussion

A human metaphase chromosome was selected by light microscopy for UV-laser microdissection. After laser ablation and AFM imaging, a neighboring chromosome was dissected mechanically with the joystick-steered AFM. In the topographic AFM image (raw image,

leveled, median filtered, 500×511 pixel^2, Fig. 2a) the different cuts were prominent and could be analyzed. The structures of interest in the image had lateral dimensions of approximately 200–400 nm and exhibited a peak-to-valley difference of about 500 nm. Nominally, the AFM tip had a characteristic length scale that was about one magnitude smaller, i.e. a tip radius of 20 nm, which was comparable to the pixel-to-pixel distance of 24 nm in the image. Thus, the lateral resolution in AFM imaging was sufficient to provide reliable data for the measurement of distances in the image.

This was proven by image analysis. A blind tip-estimation algorithm was used for the estimation of the tip dimensions from the image data. The tip characterization yielded a numerical estimate for the tip as shown in Fig. 2b. The aspect ratio of this worst-case estimate for the tip geometry indicated that the duality of the AFM tip was acceptable for the given resolution. In Fig. 2a the corresponding certainty map is superimposed on the raw image data. Certain topographic raw data are shown in light gray. Assuming the tip in Fig. 2b, the true topography could be reconstructed for these certain pixels. Pixels marked in black correspond to areas where a reconstruction with the tip (Fig. 2b) was uncertain, i.e. the reconstructed surface was not necessarily equal to the true topography. Image data in the area of the AFM cut as well as a few pixels at the edges of the laser cut were uncertain (arrows). The remaining 99.6% of the image were certain.

With this information, an image restoration was performed. Figure 3a shows the reconstructed image. Note that the aim of this analysis procedure was to provide a reliable upper limit for the lateral dimensions of depressions in the surface, as it is necessary for the investigation of the quality of laser and AFM nanodissection. This differs from the direct analysis of raw data without further image processing, which only can provide lower estimates.

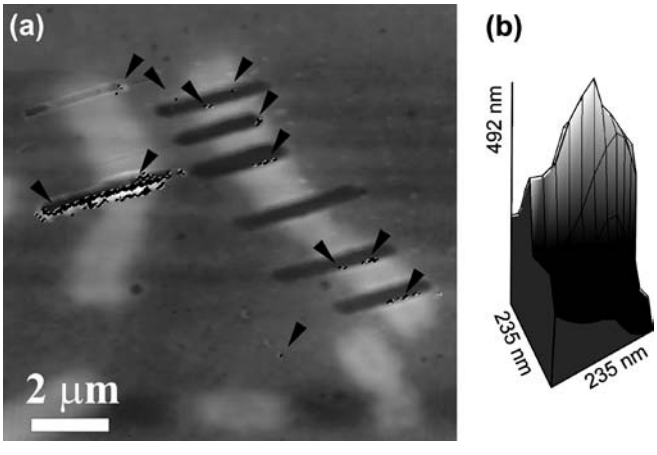

Fig. 2 a Reliable data of the raw topographic image (*light gray*). *Black pixels* indicate uncertain data. For better perception of uncertain pixels they are surrounded by a *black/white boundary* and are marked by *arrows*. **b** AFM tip as reconstructed by the blind tip-estimation

The chromosome in Fig. 3a (right) was dissected with the UV laser adjusted to a pulse energy of 0.7 μJ at the specimen at a repetition rate of 60 Hz and a scan speed of 0.3 μm/s. From the AFM data it was identified as chromosome no. 2 (measured length $L = 9.2$ μm and centromere index $CI = 39.4 \pm 1.0$). A cut width of 380 ± 20 nm (full width at half maximum cut depth) could be achieved in cut no. UV1. The chromosome was fully dissected and the cut reaches down to the substrate with a sidewall angle of 60°. The laser cuts nos. UV1 and UV2 are separated by 850 ± 45 nm and a 420-nm wide chromosomal fragment remained in between. Thus, with the UV-laser beam, sharp and precise cuts could be obtained, where the entire chromosomal material within the cut was ablated. The steep sidewalls of the cuts indicate that very precise cuts can be performed in chromosomal material, which is necessary to isolate small regions of interest. The question if the remaining chromosomal material close to the cut region is genetically intact after possible UV irradiation cannot directly be answered by microscopic methods. However, from

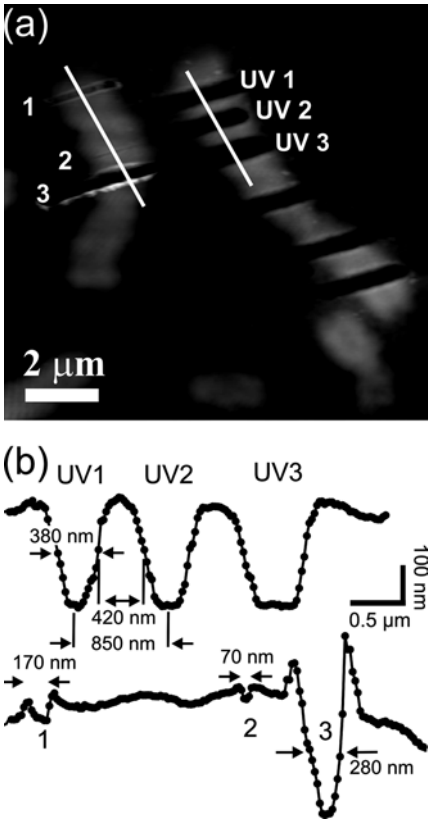

Fig. 3 a Restored topographic AFM image of manipulated human metaphase chromosomes. In order to estimate the cut-widths correctly, an image restoration was performed assuming an AFM tip as obtained by the blind tip-estimation. The chromosome on the *right* was manipulated using the UV-laser microbeam. The chromosome on the *left* was dissected by the AFM (loading forces: *1*, 20 μN; *2*, 10 μN; *3*, 40 μN). **b** Cross-sectional analysis as indicated

the height-profile measurement (Fig. 3b) it is clear that the height of the remaining fragment between both laser cuts nos. UV1 and UV2 remains unchanged. In comparison with earlier results (Thalhammer et al. 1997b), the minimum cut size for chromosomal nanodissection by UV-laser manipulation could be reduced significantly from 650 nm to a size of 380 nm.

For AFM nanodissection a medium-sized submetacentric chromosome was selected ($L = 6.2$ μm, $CI = 40.5 \pm 1.4$). With the AFM, different cut depths could be realized. At a loading force of 10 μN of the tip onto the sample, a shallow scratch with a cut depth of 20 nm and a cut width of 70 nm could be realized (Fig. 3, cut no. 2). With an increased loading force of 20 μN, a 50 nm deep and 170 nm wide cut was achieved (no. 1). At forces of 40 μN the chromosome was fully dissected (no. 3). However, the uncertain pixels of the image restoration had to be accounted for in the estimation of the cut width. As determined from the restored image (Fig. 3), the cut width was 280 nm, which is an upper limit. The lower limit of 240 nm was determined directly from the raw data (Fig. 2). Biological material was deposited by the plowing tip next to the cuts. It can be expected that part of the material is adhering to the AFM tip after dissection (Thalhammer et al. 1997a; Stark et al. 1998).

Figure 4 shows a metacentric human metaphase chromosome (no. 3; $L = 7.9$ μm, $CI = 47.7 \pm 1.4$) where three UV-laser cuts were performed using the force-feedback joystick. The pulse energy was adjusted to 0.5 μJ and the pulse repetition rate to 60 Hz. For dissection the chromosome was moved once through the laser focus at a velocity of about 0.5 μm/s. With cut no. 1 the chromosome was successfully dissected, whereas in cut no. 2 remnants of the biological material remained. For cut no. 3 the manipulation resulted in small holes in the material.

A closer investigation of Fig. 4 illustrates the necessity to examine the quality of AFM images thoroughly in order to allow for a reliable analysis of lateral dimensions of the structures created by nanomanipulation. The topographic AFM (512×512 pixel^2) image of the UV-laser dissected chromosome in Fig. 4a was leveled and subsequently filtered by a 3×3 median filter. A cross-sectional analysis (Fig. 3c) gives a lower estimate for the cut width of 330 ± 20 nm for cut no. 1. However, the blind tip-estimation reveals a blunt tip, as shown in Fig. 4e. Thus, a significant deterioration of the AFM image can be expected. Figure 4b shows the restored topographic image with increased cut widths. From these data an estimate for the cut width of 500 ± 25 nm is achieved (Fig. 4d), indicating a not perfectly adjusted UV-laser beam.

This example shows that for quality control of nanomanipulation of biological specimens, AFM data obtained with a dull tip like in Fig. 4e has to be rejected. In practice the AFM tip should be replaced and the measurement should be repeated. This corresponds to the procedure of tip quality control, as is already successfully implemented for industrial robot AFMs operating in semiconductor fabrication lines.

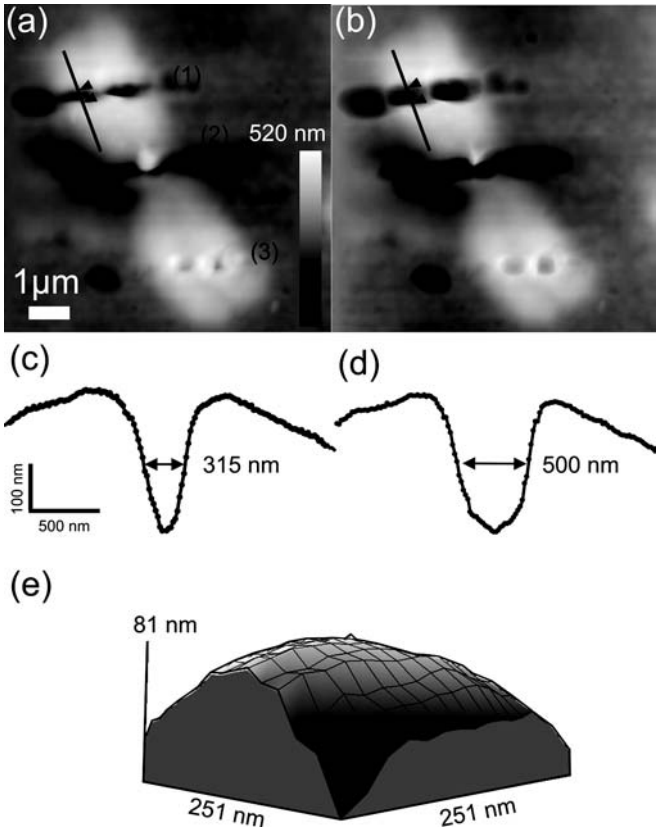

Fig. 4 a Topographic AFM image of a human metaphase chromosome (no. 3) that was microdissected with the UV laser. **b** The same image after image restoration. **c**, **d** Cross-section analysis for the laser cut in the respective images above. Note that the width of the depression can significantly be underestimated without image reconstruction. **e** Three-dimensional representation of the estimated AFM tip

Conclusions

Chromosomal dissection with cut widths close to the diffraction limit of the light microscope could be achieved by optical manipulation with a UV laser as well as by mechanical manipulation with the AFM. This clearly shows that for the diagnostics of UV-laser microbeam ablation an AFM is an indispensable tool. However, modern image processing tools like blind tip-estimation and image restoration are required to obtain reliable metrological data.

The results show the resolution capability of UV-laser ablation. With a standard nitrogen laser system a cut width less than 380 nm is possible in human metaphase chromosomes. This is an important requirement for the generation of genetic probes by microdissection for high-resolution cytogenetic analysis. Highly resolving dissection can be achieved with an integrated microscope that allows for precise mechanical mi-

cromanipulation by the AFM as well as optical manipulation by UV-laser microbeam ablation. The cuts can directly be characterized in situ by atomic force microscopy. Additionally, the scanning tip of the AFM can easily be used for micromanipulation with sub-wavelength resolution.

Thus, a semi-automated nanodissection environment is feasible, where the operator performs the dissection using a haptic interface. The quality of the dissection tip can be controlled automatically by blind tip-estimation routines. A crucial task in an automated environment is the identification of the chromosomes from scanning probe data. In order to allow for unequivocal classification, SPM analysis of banding or fluorescent labeling is required. Although the classification can be done manually for banded chromosomes (Thalhammer et al. 2001), computer-based procedures (Lerner 1998) will further facilitate chromosomal nanodissection.

Acknowledgements We thank Triple-O GmbH, Potsdam, Germany for technical support. Financial support by BMB + F, grant number 13N7509/1, is gratefully acknowledged.

References

Allen MJ, Lee C, Lee JDT, Pogany GC, Balooch M, Siekhaus WJ, Balhorn R (1993) Atomic-force microscopy of mammalian sperm chromatin. Chromosoma 102:623–630

Bäuerle D (2000) Laser processing and chemistry, 3rd edn. Springer, Berlin Heidelberg New York

Berns MW, Olson RS, Rounds DE (1969) In vitro production of chromosomal lesions with an argon laser microbeam. Nature 221:74–75

Clement Sengewald A, Buchholz T, Schütze K (2000) Laser microdissection as a new approach to prefertilization genetic diagnosis. Pathobiology 68:232–236

De Grooth BG, Putman CAJ (1992) High-resolution imaging of chromosome-related structures by atomic-force microscopy. J Microsc 168:239–247

Dongmo S, Troyon M, Vautrot P, Delain E, Bonnet N (1996) Blind restoration method of scanning tunneling and atomic-force microscopy images. J Vac Sci Technol B 14:1552–1556

Emmert Buck MR, Bonner RF, Smith PD, Chuaqui RF, Zhengping Z, Goldstein SR, Weiss RA, Liotta LA (1996) Laser capture microdissection. Science 274:998–1001

Endlich N, Harim A, Greulich KO (1994) Microdissection of single DNA molecules and DNA-polycation complexes with a UV-laser microbeam in a classical light microscope. Exp Tech Phys 40:87–93

Fritzsche W, Martin L, Dobbs D, Jondle D, Miller R, Vesenka J, Henderson E (1996) Reconstruction of ribosomal subunits and rDNA chromatin imaged by scanning force microscopy. J Vac Sci Technol B 14:1405–1409

Godstein SR, Pohida T, Smith PD, Peterson JI, Wellner E, Malekafzali A, Suarez Qian CA, Bonner RF (1999) An instrument for performing laser capture microdissection of single cells. Rev Sci Instrum 70:4377–4385

Greulich KO (1999) Micromanipulation by light in biology and medicine: the laser microbeam and optical tweezers. Birkhäuser, Basel

Greulich KO, Pilarczyk G, Hoffmann A, Meyer Zu Horste G, Schafer B, Uhl V, Monajembashi S (2000) Micromanipulation by laser microbeam and optical tweezers: from plant cells to single molecules. J Microsc 198:182–187

Guthold M, Falvo M, Matthews WG, Paulson S, Mullin J, Lord S, Erie D, Washburn S, Superfine R, Brooks FP Jr, Taylor RM II (1999) Investigation and modification of molecular structures with the nanoManipulator. J Mol Graph Mod 17:187–197

Henderson E (1992) Imaging and nanodissection of individual supercoiled plasmids by atomic-force microscopy. Nucleic Acids Res 20:445–447 [erratum in Nucleic Acids Res (1992) 20:1841]

Hillner PE, Radmacher M, Hansma PK (1995) Combined atomic-force and scanning reflection interference contrast microscopy. Scanning 17:144–147

Jondle DM, Ambrosio L, Vesenka J, Henderson E (1995) Imaging and manipulating chromosomes with the atomic-force microscope. Chromosome Res 3:239–244

König K, Riemann I, Fritzsche W (2001) Nanodissection of human chromosomes with near-infrared femtosecond laser pulses. Opt Lett 26:819–821

Krautbaur R, Clausen-Schaumann H, Gaub HE (2000) Cisplatin changes the mechanics of single DNA molecules. Angew Chem Int Ed 39:3912–3915

Lerner B (1998) Toward a completely automatic neural-network-based human chromosome analysis. IEEE Trans Sys Man Cyber B 28:544–552

Markiewicz P, Goh MC (1995) Atomic-force microscope tip deconvolution using calibration arrays. Rev Sci Instrum 66:3186–3190

McMaster TJ, Hickish T, Min T, Cunningham D, Miles MJ (1994) Application of scanning force microscopy to chromosome analysis. Cancer Genet Cytogenet 76:93–95

Perkins TT, Quake SR, Smith DE, Chu S (1994) Relaxation of a single DNA molecule observed by optical microscopy. Science 264:822–826

Putman CAJ, Van Leeuwen AM, De Grooth BG, Radosevic K, Van Der Werf KO, Van Hulst NF, Greve J (1993) Atomic-force microscopy combined with confocal laser scanning microscopy: a new look at cells. Bioimaging 1:63–70

Rasch P, Wiedemann U, Wienberg J, Heckl WM (1993) Analysis of banded human chromosomes and in situ hybridization patterns by scanning force microscopy. Proc Natl Acad Sci USA 90:2509–2511

Rubio-Sierra FJ, Stark RW, Thalhammer S, Heckl W (2003) Force feedback joystick as a low cost haptic interface for an atomic-force microscopy nanomanipulator. Appl Phys A (in press)

Sader JE, Chon JWM, Mulvaney P (1999) Calibration of rectangular atomic-force microscope cantilevers. Rev Sci Instrum 70:3967–3969

Schermelleh L, Thalhammer S, Heckl W, Pösl H, Cremer T, Schütze K, Cremer M (1999) Laser microdissection and laser pressure catapulting for the generation of chromosome-specific paint probes. Biotechniques 27:362–367

Schütze K, Becker I, Becker KF, Thalhammer S, Stark R, Heckl WM, Bohm M, Pösl H (1997) Cut out or poke in – the key to the world of single genes: laser micromanipulation as a valuable tool on the look-out for the origin of disease. Genet Anal 14:1–8

Srinivasan R (1986) Ablation of polymers and biological tissue by ultraviolet-lasers. Science 234:559–565

Stark RW, Thalhammer S, Wienberg J, Heckl WM (1998) The AFM as a tool for chromosomal dissection – the influence of physical parameters. Appl Phys A 66:S579–S584

Tamayo J, Miles M, Thein A, Soothill P (1999) Selective cleaning of the cell debris in human chromosome preparations studied by scanning force microscopy. J Struct Biol 128:200–210

Thalhammer S, Stark RW, Müller S, Wienberg J, Heckl WM (1997a) The atomic-force microscope as a new microdissecting tool for the generation of genetic probes. J Struct Biol 119:232–237

Thalhammer S, Stark RW, Schütze K, Wienberg J, Heckl WM (1997b) Laser microdissection of metaphase chromosomes and characterization by atomic-force microscopy. J Biomed Opt 2:115–119

Thalhammer S, Koehler U, Stark RW, Heckl WM (2001) GTG banding pattern on human metaphase chromosomes revealed by high resolution atomic-force microscopy. J Microsc 202:464–467

van Loenen EJ, Dijkkamp D, Hoeven AJ, Lenssinck JM, Dieleman J (1990) Evidence for tip imaging in scanning tunneling microscopy. Appl Phys Lett 56:1755–1757

Villarrubia JS (1997) Algorithms for scanned probe microscope image simulation, surface reconstruction, and tip estimation. J Res Natl Inst Stand Technol 102:425–454

Vogel F, Motulsky AG (1997) Human genetics: problems and approaches, 3rd edn. Springer, Berlin Heidelberg New York

Xu XM, Ikai A (1998) Retrieval and amplification of single-copy genomic DNA from a nanometer region of chromosomes: a new and potential application of atomic-force microscopy in genomic research. Biochem Biophys Res Commun 248:7440–748